# Between Lives and Economy: COVID-19 Containment Policy in Open Economies*

Wen-Tai Hsu† Hsuan-Chih (Luke) Lin‡ Han Yang§

December 30, 2021

**Abstract**

This paper studies containment policies for combating a pandemic in an open-economy context. It does so via quantitative analyses using a model that incorporates a standard epidemiological compartmental model in a general equilibrium multi-country, multi-sector Ricardian model of international trade. We devise a novel approach in computing national policies in the long run and contrast these policies with a baseline in which countries maintain their current policies until there is sufficient vaccine rollout. We find that (1) international trade acts as a buffer against welfare losses during the pandemic and lowers the number of cumulative infection cases and deaths; (2) the optimal containment policies greatly differ across countries: while most countries should tighten pandemic restrictions, some countries should ease them, depending on their epidemiological and trade factors; (3) compared to the case of autarky, the optimal policy with trade is generally more stringent, because trade allows countries to save more lives without greatly reducing domestic production.

**Keywords:** COVID-19, pandemic, welfare analysis, disease dynamics, effective reproduction number, containment policy, optimal policy, open economy, trade

**JEL Classification:** I18; F11; F40; E27

*We thank Ippei Fujiwara, Taiji Furusawa, Matt Shapiro, Michael Zheng Song, and seminar participants in Asia Pacific Trade Seminars, Academia Sinica, Singapore Management University, and the Virtual East Asia Macroeconomic Seminar Series. The online appendix to this paper is available at http://wthsu.com.

†School of Economics, Singapore Management University. Email: wentaihsu@smu.edu.sg.

‡Institute of Economics, Academia Sinica, Taiwan. Email: linhc@econ.sinica.edu.tw.

§Institute of Economics, Academia Sinica, Taiwan. Email: hanyang@econ.sinica.edu.tw.

# 1 Introduction

One of the most important questions in a major pandemic, such as the COVID-19 one we face now, is how stringent the containment policies should be. There are heated debates on this in many countries, and a large cross-country variation in the stringency of containment policies is apparent. The key trade-off is obvious: lives vs. economy. But striking the right balance is not a simple task due to the complexity of the economy and its complicated interaction with the disease's epidemiological evolution. There has been a surge of research on containment policy in macroeconomics literature, but these studies are mostly, if not all, in closed-economy contexts. As the global economy is interlinked across countries, a country's containment policy may have repercussions on other countries' economies through various trade linkages, which may, in turn, affect the considerations of other countries' containment policies and the ensuing health outcomes.

This paper attempts to answer questions regarding containment policy in an open-economy context. We do so by conducting quantitative analyses using a model that incorporates a standard epidemiological compartmental model (**S**usceptible-**I**nfected-**R**ecovered-**D**eceased; SIRD) in a multi-country, multi-sector Ricardian model of international trade. In particular, our model builds on that of Eaton and Kortum (2002) by adding how the pandemic shocks different sectors and countries differently due to the heterogeneity in containment policy and work-from-home (henceforth WFH) capacity, which in turn reshapes comparative advantages and the distribution of sectoral employment. The rate of disease transmission is then influenced by such changes in sectoral employment through workplace interactions, and the SIRD law of motion then influences the next-period labor supply. Thus, this model features two-way dynamic influences between the economy and the pandemic. It also features cross-country externality of containment policies through trade linkages.

We calibrate our model to the pre-COVID-19 economy by mainly using the World Input-Output Database (WIOD), in which there are 41 countries. Our key disease transmission parameters are disciplined by data on the total deaths from COVID-19. Using the calibrated model, we conduct various counterfactual analyses. To consider the long-run effects of containment policies, we first simulate a baseline model in which countries retain their current policies until the pandemic ends with sufficient vaccination being rolled out. Our welfare measure is equivalent to the sum of individual expected utilities, which are concerned with risks in a pandemic, as, ex ante, no one knows how he/she would face during the pandemic. Under general risk aversion, people dislike extreme outcomes; hence, an increase in the probability of death or infection worsens welfare beyond the loss in real income.

Our analysis consists of three parts. In the first part, we analyze the role of international trade under the COVID-19 pandemic. In particular, we compare the losses in welfare and real income during the pandemic with and without international trade. Our results show that with international trade, losses in welfare and real income are both smaller than the case under autarky for the whole world. However, a large extent of heterogeneity is observed across countries: 6 out of 41 countries actually incur higher losses with trade than under autarky. This result is striking and yet implies that there exists no universal rule that all the countries can follow. With respect to the cumulative numbers of confirmed cases and deaths, we observe that both numbers are much smaller with trade than in autarky, implying that trade can help the countries to "*flatten the curve*" of the pandemic.

In the second part, because substantial heterogeneities are observed across countries, we analyze the optimal containment policy that maximizes the expected discounted total utility for each country. When computing optimal policies in such a multi-country, multi-sector, multi-period framework, the key challenge is to devise a reasonable and tractable approach to reduce the space of candidate policies. To facilitate efficient computation of optimal policies, we use the effective reproduction number $R_e$ as the policy target for each country instead of optimizing over the entire time paths of policies for all countries. Setting a cap of the effective reproduction number is in fact a reasonable target/representation, as $R_e$ reflects the speed of disease spread and is the central concern for epidemiologists and doctors who lead government responses. Such a characterization of the model also leads to the implications consistent with recent studies in the macroeconomic literature that find that containment measures should be stringent initially and generally become more lenient over time. While the existing macroeconomic studies focus on the dynamics of optimal policies in closed-economy contexts (see, e.g., Alvarez et al. (2021) and Jones et al. (2021)), we study the optimal containment policy in the context of an open economy.

To further reduce the computational burden, we compute optimal policies in two steps. In the first step, we consider a global planner who seeks to maximize global welfare by deciding on an $R_e$ that applies to all countries. The result of this step serves as the starting point to compute the optimal deviations of each country. In the second step, we solve each country's ($i$) optimal effective reproduction number $R_{e,i}$ given other countries' optimal choices $R_{e,-i}$; this is, indeed, a Nash equilibrium of national optimal policies. Information from the first step helps to ease the computational burden in this step as it suggests how the grid search can be efficiently conducted.

The results show that the optimal policy target for a majority of countries is to tighten restrictions to the extent that the disease will naturally disappear (i.e., $R_{e,i} < 1$), whereas, for some countries (7 out of 41 countries), the optimal target is not low enough to eliminate the disease ($R_{e,i} > 1.3$). The key reasoning behind such heterogeneity is the following. When a country con-

siders a stringent containment policy that targets a sufficiently low $R_{e,i}$, lives versus economy is the main welfare trade-off. Therefore, there exists a local maximum for each country and deviating from the local maximum leads to lower welfare. However, when the containment policy is already relaxed (i.e., when the policy is closer to laissez-faire), relaxing the restrictions even further results in lower welfare for most countries but in higher welfare for a few countries. Which group a country belongs to depends on the factors related to epidemiological and international trade factors.

In the third part, we analyze the role of international trade by comparing the optimal containment policies with and without trade. We find that with international trade, most countries' optimal containment policies are stricter than the case under autarky. This implies that, under the optimal policies, the cumulative numbers of confirmed cases and deaths are smaller with international trade than in autarky. This result is intuitive because international trade acts as a buffer such that countries can implement a more extreme containment measure without greatly reducing domestic production. The average difference in welfare improvement under optimal policies between closed and open economies is 45% relative to the welfare improvement in open economies.

We also discuss the limitations of our model. The counterfactual analyses, including the one for the optimal policies, are based on several model assumptions. We check whether the implications are sensitive to certain specifications. First, our model is built on Eaton and Kortum (2002) instead of Caliendo and Parro (2015). The main difference is that we intentionally leave the input-output linkages (I-O) out from our benchmark in order to highlight the importance of international trade. To check the robustness, we re-conduct the analysis using the framework of Caliendo and Parro (2015) and find that the results are qualitatively similar, although the magnitude of the importance of international trade is larger with input-output linkages. Second, we simulate our results by changing the values of several epidemiological parameters. We find that, among model parameters, the results are relatively more sensitive to the basic reproduction number, but the main implications remain similar. Thus, our analysis is informative even when we face a different pandemic—as long as the pandemic is not very different in terms of the basic reproduction number—since we would reach the same conclusion that international trade could play an important role in combating a pandemic.

*Relevance to the literature.* There has been a surge of research studying optimal containment policies: these studies embed variants of the classic SIR model proposed by Kermack et al. (1927) into macroeconomic models to study various aspects of the tradeoff between lives and economy. See, for examples, Acemoglu et al. (2021), Alvarez et al. (2021), Atkeson (2020), Atkeson et al.

(2021), Eichenbaum et al. (2021), Farboodi et al. (2021), Jones et al. (2021), Krueger et al. (2020), and Piguillem and Shi (2020). Our work differs from all of the above in our focus on analyzing optimal containment policies in an open-economy context. A particularly closely related work is that by Budish (2020), who formulates a static optimization problem using $R_e < 1$ as a constraint. Our work differs as $R_e$ is used as a policy target (rather than a constraint) in a dynamic setting.

Also closely related are the studies by Antràs et al. (2020), Fajgelbaum et al. (2021), and Argente et al. (2021), who all consider disease dynamics in a general equilibrium model of trade in either a city or an international-trade setting. Our work differs from Antràs et al. (2020) mainly due to our focus on optimal containment policies, and it differs from Fajgelbaum et al. (2021) and Argente et al. (2021) due to our focus on country-level containment policies. Broadly related work includes Chen et al. (2020), Bonadio et al. (2021), and Eppinger et al. (2020), who study the role of trade and/or input-output linkages in the pandemic's shocks on the economy. However, these studies do not incorporate disease dynamics or analyze optimal containment policies, which are our main focuses.

The rest of the paper is organized as follows. Section 2 describes the model, Section 3 introduces the data and how the model is calibrated, Section 4 presents the quantitative analyses on containment policies, and Section 5 concludes.

## 2 Model

Our model incorporates the evolution of the pandemic and the labor productivity shocks arising from the pandemic into a general equilibrium Eaton and Kortum (2002) model with multiple sectors.

### 2.1 Preference

There are $K$ countries, each of which has a population of $N_i, i \in \{1, 2, ..., K\}$. There are $J$ sectors, each of which consists of a unit continuum of varieties. The final-good consumption of an individual in country $i$ in period $t$, $q_{i,t}$, consists of a Cobb-Douglas bundle of sectoral goods:

$$q_{i,t} = \prod_{j=1}^{J} (q_{i,t}^{F,j})^{\alpha_i^j},$$

and each sectoral good $q_{i,t}^{F,j}$ is made of a CES composite:

$$q_{i,t}^{F,j} = \left[ \int_0^1 q_{i,t}^{F,j}(\omega)^{\frac{\kappa-1}{\kappa}} d\omega \right]^{\frac{\kappa}{1-\kappa}}, \tag{1}$$

where $q_{i,t}^{F,j}(\omega)$ is the amount of variety $\omega$ used for final consumption and $\kappa > 1$ is the elasticity of substitution. The lifetime utility of an individual (in a dynastic sense) is given by

$$u_i = \sum_{t=0}^{\infty} \rho^t u\left(q_{i,t}\right),$$

where $\rho$ is the discount factor and $u$ is a concave and strictly increasing function.

## 2.2 Production

Labor is the fundamental input for production. Countries differ in their productivities across sectors and varieties. Production technology exhibits constant returns to scale. Both the goods and factor markets are perfectly competitive.

Denote a country-sector-time-specific pandemic shock parameter on the production function by $B_{i,t}^j$, which will be specified later; for the pre-COVID-19 economy, this term drops out as $B_{i,t}^j = 1$. The production function of a variety $\omega$ in sector $j$ and country $i$ is given by

$$y_{i,t}^j(\omega) = z_i^j(\omega)\left[B_{i,t}^j L_{i,t}^j(\omega)\right], \tag{2}$$

where $L_{i,t}^j(\omega)$ is the labor hired for this variety and the Hicks-neutral productivity $z_i^j(\omega)$ is drawn *i.i.d.* from a Fréchet distribution: $\Pr(x < z) = \exp(-T_i^j z^{-\theta})$, where $T_i^j > 0$ is the country-sector-specific scaling parameter and $\theta > 1$ is the shape parameter. The draws are also independent across countries and sectors.

The trade cost is of the standard iceberg-cost form: to deliver one unit of sector-$j$ variety from country $i$ to country $n$, $\tau_{i,n}^j \geq 1$ units are required to ship. We assume that trade is balanced. The unit cost of delivering a good from country $i$ to country $n$ is $c_{i,t}^j \tau_{i,n}^j / z_{i,t}^j(\omega)$; since labor is the only input of production,

$$c_{i,t}^j = \left(\frac{w_{i,t}}{B_{i,t}^j}\right),$$

where $w_{i,t}$ is country $i$'s wages. Here, $c_{i,t}^j$ is indeed the unit cost to produce a sector $j$ variety under unit productivity. In this environment with perfect competition and constant returns to scale, prices equal the (delivered) marginal costs, and each country $n$ buys from the cheapest source: $p_{n,t}^j(\omega) = \min_i \left\{c_{i,t}^j \tau_{i,n}^j / z_{i,t}^j(\omega)\right\}$. Standard derivations yield the price indices:

$$P_{i,t}^j = \left(\int_0^1 p_{i,t}^j(\omega)^{1-\kappa}\right)^{\frac{1}{1-\kappa}}, \quad P_{i,t} = \prod_{j=1}^{J}\left[P_{i,t}^j\right]^{\alpha_i^j}. \tag{3}$$

### 2.3 Pandemic and Economy

We incorporate a standard epidemiological model, i.e., an SIRD model, as follows. At any period $t$, the population of country $i$, $N_i$, consists of people who are **S**usceptible ($S_{i,t}$, have not been exposed to the disease), **I**nfectious ($I_{i,t}$, have contracted the disease), **R**ecovered ($R_{i,t}$, have recovered and are immune), and **D**eceased ($D_{i,t}$, died from the disease). That is, $N_i = S_{i,t} + I_{i,t} + R_{i,t} + D_{i,t}$. The epidemiology is characterized by

$$\begin{aligned} S_{i,t+1} &= S_{i,t} - T_{i,t} \\ I_{i,t+1} &= I_{i,t} + T_{i,t} - (\pi^r + \pi^d_{i,t}) I_{i,t} \\ R_{i,t+1} &= R_{i,t} + \pi^r I_{i,t} \\ D_{i,t+1} &= D_{i,t} + \pi^d_{i,t} I_{i,t}, \end{aligned}$$

where $\pi^r$ and $\pi^d_{i,t}$ are the probability of recovering from the infectious status in one period and the probability of death in period $t$, respectively, and $T_{i,t}$ is the number of newly infected people. To capture the fact that the strain of the number of infectious people on the medical system generally increases the mortality rate $\pi^d_{i,t}$, we assume $\pi^d_{i,t} = \pi^d + \delta I_{i,t}/N_i$, where $\delta > 0$ and $\pi^d$ is the base mortality rate. This linear form is also assumed by Alvarez et al. (2021).

Next, we link the SIRD model back to our economic environment. As deaths reduce the labor force and infections negatively affect individuals' labor supply, the effective labor force at time $t$ is

$$L_{i,t} = S_{i,t} + R_{i,t} + \alpha^I I_{i,t}, \tag{4}$$

where a fraction $1 - \alpha^I$ of labor time is lost from contracting the disease.

Let $\mu^j_i \in [0,1]$ be the capacity to work from home for sector $j$ in country $i$, and let $\eta_{i,t} \in [0,1]$ be the degree of the containment measure in country $i$ at time $t$; $\eta_{i,t} = 1$ means a total lockdown whereas $\eta_{i,t} = 0$ means totally laissez-faire, but a containment policy can be anywhere in between. Assume that during a pandemic, workers who can work from home (the fraction of such workers is $\mu^j_i$) work from home regardless of the containment policy, but for those workers who are unable to work from home, they must still meet in workplaces if allowed. If a country's containment measure is $\eta_{i,t}$, then a fraction $\eta_{i,t}(1-\mu^j_i)$ of workers are locked away. Only those who are not locked away still meet; the fraction of such workers is $(1-\eta_{i,t})(1-\mu^j_i)$. Assume that the containment measure also applies to interactions in general activities. The number of newly infected individuals is given by

$$T_{i,t} = \frac{(1-\eta_{i,t})\pi^I_i S_{i,t} I_{i,t} + \pi^L_i \times \sum_{j=1}^{J} \left[(1-\eta_{i,t})(1-\mu^j_i)\ell^j_{i,t}\right] S_{i,t} I_{i,t}}{N_i}, \tag{5}$$

where $\ell_{i,t}^j$ is sector $j$'s employment share in country $i$ at time $t$, and $\pi_i^L$ and $\pi_i^I$ are the infection rates from interactions at workplaces and from general activities other than working, respectively. Similar forms have been used in Eichenbaum et al. (2021) and Jones et al. (2021). The key difference between our study and these macroeconomic models is that instead of focusing on how households react to the pandemic by cutting their consumption and labor supply, we expand in the country and sector dimensions to study how sectoral employment shares $\{\ell_{i,t}^j\}$ react to changing circumstances of containment policies, augmented by the sectoral WFH capacity, and subsequently affect the speed of disease spread.

As the effective labor time supplied per worker in sector $j$ and country $i$ is reduced to $\mu_i^j + (1-\eta_{i,t})(1-\mu_i^j) = 1-\eta_{i,t}(1-\mu_i^j)$, the employers can pay the full wages even when workers' effective time supplied is reduced or they can choose to lay off workers or hire part-time. In the former case, employers absorb the shocks directly, whereas the workers absorb the shocks in the latter case. Both scenarios are present in reality, and their effects are similar. To keep the model tractable, we focus on the former case. Thus, the pandemic-shock parameter in the production function (20) is $B_{i,t}^j \equiv 1-\eta_{i,t}(1-\mu_i^j) \in [0,1]$. In the case where $\eta_{i,t}=0$ (as would be the case when there is no pandemic or when a laissez-faire policy is adopted), $B_{i,t}^j = 1$.

Observing (20) and (5), a more stringent containment measure (higher $\eta_{i,t}$) reduces infections but hurts production; both effects are mitigated if the sector of concern has a larger WFH capacity. Both effects also differ across countries due to the differences in infection probabilities $\{\pi_i^I, \pi_i^L\}$ and country-specific production parameters. The international division of labor reflected by $\{\ell_{i,t}^j\}$ provides an *endogenous source* of cross-country heterogeneity in the rate of transmission. We allow for $\pi_i^I$ and $\pi_i^L$ to differ across countries because these may reflect country-specific environments, such as geography, climate, or culture, that potentially affect the rate of disease transmission given the same intensity of interactions in workplaces and in general.

Assuming $\kappa < \theta + 1$, the price index of a sectoral good is given by

$$P_{n,t}^j = \zeta \left( \sum_{k=1}^{K} T_k^j \left[ \left( w_{k,t}/B_{k,t}^j \right) \tau_{k,n}^j \right]^{-\theta} \right)^{-\frac{1}{\theta}}, \tag{6}$$

where $\zeta \equiv \left[\Gamma\left(\frac{\theta+1-\kappa}{\theta}\right)\right]^{1/(1-\kappa)}$, and the expenditure share of sector-$j$ goods that country $n$ purchases from country $i$ is given by

$$\pi_{i,n,t}^j = \frac{T_i^j \left[ \left( w_{i,t}/B_{i,t}^j \right) \tau_{i,n}^j \right]^{-\theta}}{\sum_{k=1}^{K} T_k^j \left[ \left( w_{k,t}/B_{k,t}^j \right) \tau_{k,n}^j \right]^{-\theta}}. \tag{7}$$

Containment policies combined with WFH capacity reshape comparative advantages. If all countries adopt the same containment policy, a country $i$ gains a comparative advantage in those

high $\mu_i^j$ sectors as the corresponding $B_{i,t}^j$'s are larger. This means that a country's containment policy affects its *own and other* countries' distributions of sectoral employment. Subsequently, their rates of disease spread change, thus affecting the labor supply (and hence wages and comparative advantages) in the next period. Such a cross-country externality of containment policies cannot be captured in a closed-economy model. Moreover, this model is not a Caliendo-Parro model repeatedly shocked by a disease evolution that runs independently. Instead, it features a dynamic mechanism in which the economic situations also change the speed of disease spread.

### 2.4 Equilibrium

Let $R_{i,t}^j$ denote the total revenue of country $i$'s sector $j$, $X_{n,t}^j$ denote the total expenditure of country $n$ on goods in sector $j$, and $X_{n,t}$ denote the total expenditure of country $n$. By definition, $R_{i,t}^j = \sum_{n=1}^K \pi_{i,n,t}^j X_{n,t}^j$. The market clearing condition for labor is therefore

$$w_{i,t}L_{i,t} = \sum_{j=1}^J R_{i,t}^j = \sum_{j=1}^J \sum_{n=1}^K \pi_{i,n,t}^j X_{n,t}^j. \tag{8}$$

By the definition of $X_{i,t}^j$,

$$X_{i,t}^j = \alpha_i^j w_{i,t} L_{i,t}. \tag{9}$$

A brief description of the equilibrium algorithm is given as follows; the detailed algorithm is relegated to the online appendix.[1] We first solve the equilibrium at time $t$ given the SIRD objects $\{S_{i,t}, I_{i,t}, R_{i,t}, D_{i,t}\}$ and $\{L_{i,t}\}$ from (4). Given wages $\{w_{i,t}\}$, $\{P_{i,t}, P_{i,t}^j, \pi_{i,n,t}^j, X_{k,t}^j\}$ are obtained from (21), (22), (23), and (25). Equilibrium wages are obtained from (24). In particular, sectoral employment shares are computed by $\ell_{i,t}^j = R_{i,t}^j / \sum_{l=1}^J R_{i,t}^l$. Then, the next-period SIRD objects are obtained from the law of motion specified in Section 2.3 with the number of newly infected $\{T_{i,t}\}$ given by (5).

### 2.5 Welfare

A pandemic poses uncertainty to individuals as to how one would fare in terms of the compartments $\{S_{i,t}, I_{i,t}, R_{i,t}, D_{i,t}\}$. For a country $i$, its welfare is measured by the sum of individual expected lifetime utility in which everyone's probability of falling into each compartment is given by the fraction of people in that compartment.[2] As consumption is given by real income $w_{i,t}/P_{i,t}$, the welfare of country $i$ is given by

$$U_i = \sum_{t=0}^{\infty} \rho^t \left[ (S_{i,t} + R_{i,t})\, u\left(\frac{w_{i,t}}{P_{i,t}}\right) + I_{i,t} u\left(\frac{\alpha^I w_{i,t}}{P_{i,t}}\right) + D_{i,t} u\,(0) \right].$$

[1] The online appendix is available at https://wthsu.com.

[2] Note that this probability is unconditional when viewed at time 0.

Note that the concavity of $u$ reflects the degree of risk aversion. This formulation treats an individual's death as a complete loss of labor, which implies zero income and hence zero consumption. If $u(0) = 0$, then the loss from death is simply the loss of utility from the other two outcomes before one's death. When $u(0) \neq 0$, its value actually reflects the psychological cost that one may have toward death. As it is difficult to calibrate psychological costs, we set $u(0) = 0$ for a relatively clear benchmark. In most cases, it is easy to predict the directions of how our results would change when psychological costs are incorporated.

When $u$ is linear, i.e., the risk-neutral case, a country $i$'s welfare actually becomes the present value of aggregate real income: $U_i = \sum_{t=0}^{\infty} \rho^t \frac{w_{i,t} L_{i,t}}{P_{i,t}}$. The global welfare is defined analogously:

$$U = \sum_{i=1}^{K} U_i = \sum_{i=1}^{K} \sum_{t=0}^{\infty} \rho^t \left[ (S_{i,t} + R_{i,t})\, u\left(\frac{w_{i,t}}{P_{i,t}}\right) + I_{i,t} u\left(\frac{\alpha^I w_{i,t}}{P_{i,t}}\right) + D_{i,t} u\left(0\right) \right]. \tag{10}$$

As $U_i$ is already the aggregate welfare that takes into account the population in country $i$, the global welfare is simply the sum of individual countries' welfare.

# 3 Calibration

This section describes how we quantify the model. We first present the calibration for the international trade model and then discuss how to calibrate the epidemiological parameters. More details of the quantification are also relegated to Appendix A.

## 3.1 International Trade

For our quantitative analyses, we set the per-period utility as

$$u(q) = \frac{(q+1)^{1-\sigma} - 1}{1-\sigma}.$$

We choose this functional form for three reasons. First, this specification is similar to the CRRA (constant relative risk aversion) utility if the term $q + 1$ is replaced with $q$. Thus, it is approximately CRRA when $q$ is large; the parameter $\sigma$ measures the degree of relative risk aversion. Second, $u(0) = 0$, which satisfies our requirement to leave psychological costs out of the model; note that the exact CRRA utility entails $\lim_{q \to 0} u(q) \to -\infty$ when $\sigma \geq 1$ and is therefore not implementable. Third, $\sigma = 0$ corresponds to the risk-neutral case. Following Low and Pistaferri (2015), the relative risk aversion $\sigma$ is set to 1.5. Following Farboodi et al. (2021), we set the annual discount rate as $0.95$; as daily data is used, $\rho = 0.95^{\frac{1}{365}} \approx 0.99986$.

The economic environment is calibrated to the world economy prior to the COVID-19 pandemic using the World Input-Output Database (WIOD) and Centre d'Études Prospectives et

d'Informations Internationales (CEPII) data. There are 41 countries in this data set. We aggregate the 56 WIOD industries into six sectors (one primary sector, three manufacturing sectors, and two service sectors distinguished by high skill and low skill). Hence, $K = 41$ and $J = 6$.

The share parameters $\{\alpha_i^j\}$ in the utility and production functions are calibrated using the input-output information in the WIOD. Given the data on trade shares and geography from the WIOD and CEPII, the model's gravity equations and hence trade costs $\{\tau_{i,n}^j\}$ can be estimated. Following Simonovska and Waugh (2014), we set the value of trade elasticity $\theta = 4$. Given trade elasticity, estimated trade costs, the share parameters $\{\alpha_i^j\}$, and data on wages obtained from the Social Economic Account in the WIOD, the productivity parameters $\{T_i^j\}$ can then be backed out using the model structure, as in Fieler (2011) and Ravikumar et al. (2019).

The values of WFH capacity $\{\mu_i^j\}$ are obtained from Dingel and Neiman (2020), who compute such capacity by occupation and then aggregate to NAICS industries. We map their 3-digit NAICS results to WIOD industries and our aggregate sectors. The containment measures $\{\eta_{i,t}\}$ are obtained from the *Stringency Index* of the Oxford COVID-19 Government Response Tracker (OxCGRT; Hale et al. 2020) at a daily frequency. This index summarizes a government's responses in terms of various closures and containment, including school and workplace closures, stay-at-home requirements, border control, and restrictions on gathering, public events, public transport, and internal movements, as well as public information campaigns.

### 3.2 Epidemiology

Next, we turn to the epidemiological parameters $\{\pi^r, \pi^d, \delta, \pi_i^I, \pi_i^L, \alpha^I, I_{i,0}\}$. Note that recovery rate $\pi^r$, death rate $\pi^d$, medical preparedness $\delta$, and reduction in productivity $\alpha^I$ are the same across countries, while $\pi_i^I$ and $\pi_i^L$, the infection rates from workplace and general activities, are country specific. We now describe how these parameter values are set.

For the parameter values that are the same across countries, we follow the choices in the literature. As in Atkeson (2020) and several other macro-SIRD models, we set $\pi^r + \pi^d = 1/18$, which means that it takes on average 18 days to either recover or die from the infection. The case mortality rate is set at $\pi^d = 0.037 \times \frac{1}{18}$. Following Alvarez et al. (2021), we set $\delta = 0.05 \times \frac{1}{18}$. As a WHO (2020) COVID-19 Situation Report indicates that asympotomatic and mild cases account for about 80% of the infections, we set $\alpha^I = 0.8$.

As for parameters that are country specific, we describe how to calibrate them. For our purpose, it is important to account for the variations in the rate of disease reproduction across countries, the key parameters for which are the two infection probabilities $\{\pi_i^I, \pi_i^L\}$ in (5). Also, for the epidemiological evolution to commence, an estimate of $I_{i,0}$ is required (as $S_{i,0} = N_i - I_{i,0}$ and $R_{i,0} = D_{i,0} = 0$); $I_{i,0}$ is generally unknown and must be estimated because the society might

be unaware of, unprepared for, or on low alert for the disease so that the number of the first few reported cases may be quite off. For each country, parameters $\{\pi_i^I, \pi_i^L, I_{i,0}\}$ are estimated by the non-linear least squares method that minimizes the squared distance in the total deaths between data and model. The data on total deaths are downloaded from the Humanitarian Data Exchange website.[3] Note that we choose to match the total deaths over time because it has been reported that there is much noise in the total numbers of confirmed cases. We have a calibrated version that is based on the total confirmed cases, and the results are qualitatively similar.

### 3.3 Calibration Results and Goodness of Fits

We now describe the calibration results and model fit. First, a key object in epidemiology is the effective reproduction number $R_{e,i,t}$, which is the number of cases directly generated from one case, is given by

$$R_{e,i,t} \equiv \frac{T_{i,t}}{I_{i,t}} \times 18 = (1-\eta_{i,t}) \left[ \pi_i^I + \pi_i^L \times \sum_{j=1}^{J} (1-\mu_i^j) \ell_{i,t}^j \right] \times 18 \times \frac{S_{i,t}}{N_i}. \tag{11}$$

Our estimated model fits the data reasonably well, as the cross-country average of normalized root-mean-square deviation (NRMSD) is $0.13$. The calibrated results are also presented in Figure 1, which shows the over-time average of both $R_{0,i,t}$ and $R_{e,i,t}$ for each country between the onset of the disease spread $t_i^*$ and November 16, 2020. There is considerable cross-country variation in the basic reproduction number with most countries ranging from 1 to 4. However, when it comes to the effective reproduction number, the variation is much smaller. Most importantly, the scale of average $R_{e,i,t}$ is much smaller than that of average $R_{0,i,t}$ with the former hovering around 1. This indicates a strong containment effort from governments across the globe in slowing disease spread. It is then clear that most governments have adopted strategies with the prospect for vaccines in mind.

To further understand the significance of $R_{e,i,t}$, note that the expression in the brackets is actually the rate of transmission (the rate of getting infected from susceptible people); when this rate is divided by the rate of leaving the infectious compartment, $1/18$, it entails the number of cases directly generated from one case at the onset of the disease and without government intervention (so $S_{i,t}/N_i = 1$ and $1-\eta_{i,t} = 1$). This is actually the famous basic reproduction number $R_0$, although in our model it is actually country specific and time-varying (denoted as $R_{0,i,t}$) due to cross-country differences in $\{\pi_i^I, \pi_i^L\, \ell_{i,t}^j\}$ and the time variability in $\ell_{i,t}^j$. Then, the effective number of cases generated directly from one case is the product of $R_{0,i,t}$ and the fraction of "effective" susceptible people given by $(1-\eta_{i,t})S_{i,t}/N_{i,t}$.

[3] See Dong et al. (2020) (`https://data.humdata.org/dataset/novel-coronavirus-2019-ncov-cases`) for data.

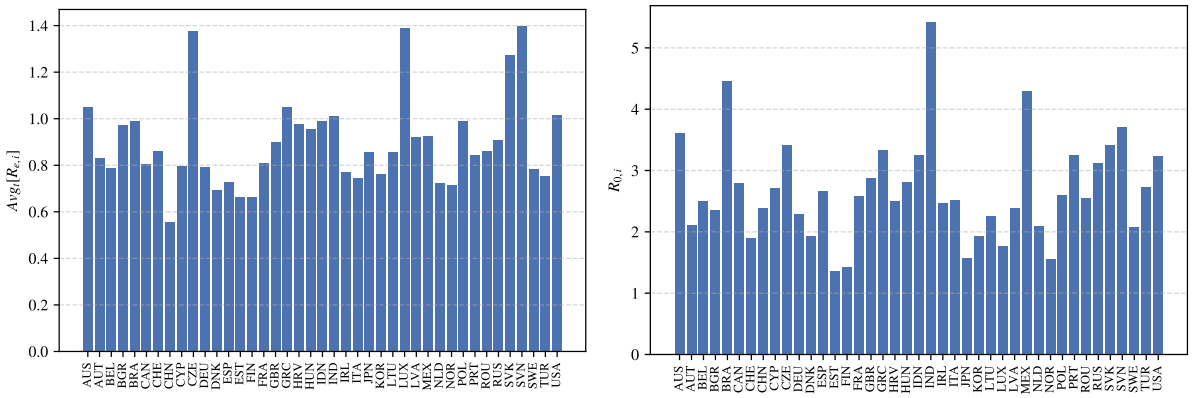


(a) Average Effective Reproduction Number $\bar{R}_{e,i}$ (b) Calibrated Basic Reproduction Number $R_{0,i}$

Figure 1: Effective Reproduction Number $\bar{R}_{e,i}$ and Basic Reproduction Number $R_{0,i}$

From (11), it is easy to understand two main strategies for combating the disease. One approach is to impose sufficiently stringent containment measures so that the effective reproduction number goes below 1, in which case the disease spread slows down, and to wait for vaccines. The second approach is to use various ways to "protect the vulnerable" while letting the disease spread faster in the hope for herd immunity. In the first approach, $1 - \eta_{i,t}$ remains low but the fraction of susceptible in the population remains high; this approach would not be feasible without reasonable prospects for vaccines in the near future. In the second approach, $1 - \eta_{i,t}$ is high, but $S_{i,t}/N_i$ goes down faster and when $S_{i,t}/N_i$ is so low that $R_{e,i,t} < 1$ even when there is no containment measure ($\eta_{i,t} = 0$), herd immunity is reached.

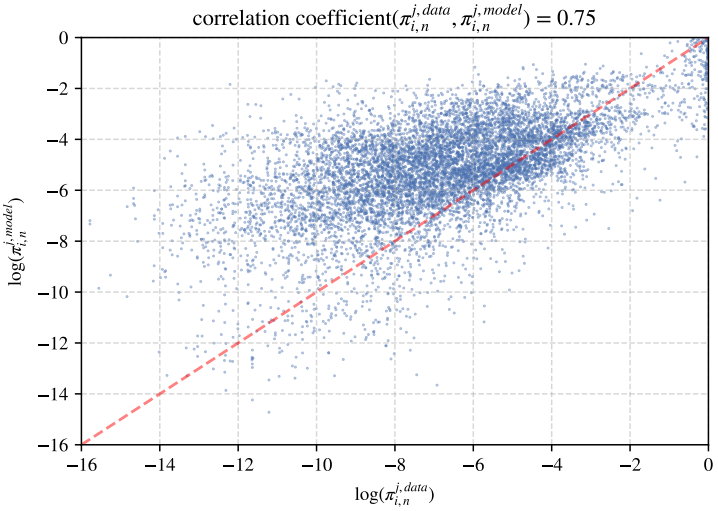


Figure 2: Bilateral Trade Fit

Finally, we demonstrate the model fit of the international trade part of our calibration. Since the main goal is to assess whether international trade may help alleviate the consequences of

a pandemic, it is important to check that our model also does a reasonable job at matching the observed cross section of international trade shares. Figure 2 plots bilateral trade shares generated using the model against the trade shares observed in the data. The correlation coefficient between the data and model is 0.75, implying that our model captures pre-pandemic trade flows reasonably well.

# 4 Counterfactual Experiments

In the previous section, we have shown the calibration results and the model fit. Using the calibrated model, we now conduct the counterfactual policy analysis in order to quantify the importance of the various channels through which international trade could affect welfare. We first analyze the role of international trade during the pandemic. We then discuss how the optimal containment policies for 41 countries can be calculated and characterize the optimal policy for each country. Finally, we discuss other possible channels and present the sensitivity analysis.

With the calibrated parameter values, we describe how we simulate the results for each counterfactual case. Note that in Section 3, we calibrated all the parameters up to November 16, 2020, and we simulate afterwards because we want to avoid complications arising from the introduction of vaccinations and dominance and replacement of various variants. For equilibrium computations, we simulate the evolution of the disease and economy from a pre-COVID-19 world with pandemic shocks $\{B^j_{i,t}\}$ from January 1, 2020 ($t = 0$). Assume that the disease evolution for a country $i$ starts at the date on which the total confirmed cases in the data exceed 50; this date is denoted as $t^*_i$. Then, the estimated $I_{i,0}$ is applied to the previous day ($t^*_i - 1$); for all days between January 1, 2020 and that previous day, $I_{i,t} = R_{i,t} = D_{i,t} = 0$ and $S_{i,t} = N_{i,t}$.

For dates after November 16, 2020, we assume each country will maintain the average effective reproduction number until $t > 730$, after which no additional COVID-19 cases are allowed and the world goes back to the steady state. Even though several vaccines have been successfully developed, how soon the pandemic will end depends on their rollout, as well as other factors. For our exercises, we assume that the pandemic ends in two years ($t = 730$) from January 1, 2020.[4] So, $\pi^N_i$ and $\pi^I_i$ are set to 0 for $t > 730$, and thus the effective reproduction number also becomes 0. Since COVID-19 would be no longer contagious, containment policies are scrapped for $t > 730$. Note that the disease evolution does not immediately end at $t = 730$, as it takes some time for infectious people to move to the next state (recovery or death).

[4]Powell A. "Fauci says herd immunity possible by fall, 'normality' by end of 2021" The Harvard Gazette, December 10, 2020, https://news.harvard.edu/gazette/ and The Lancet Microbe (2021).

### 4.1 The Role of International Trade

We first examine the role of international trade in our quantitative analysis. In particular, we examine whether trade mitigates or amplifies the losses from COVID shocks.

We begin by showing the welfare and real income losses compared to the case without a pandemic. In Figure 3, we present the welfare and real income losses from COVID shocks under trade to that under autarky. The x-axis contains country labels, and the percentage change (loss) compared to the case without a pandemic is on the y-axis. The shorter the bar, the less impact this pandemic has. In Figure 3(a), we can observe that most countries incur lower losses under trade than under autarky. Among 41 countries, only six countries (Australia (AUS), Brazil (BRA), Indonesia (IDN), India (IND), Romania (ROU), and Russia (RUS)) have a larger welfare loss under trade than under autarky. Figure 3(b), which presents real-income losses, admits similar patterns except that differences between trade and autarky cases are less. These results imply the following. First, international trade can largely help most countries to combat a pandemic, but there is no universal rule that all countries can follow. Second, there are seemingly asymmetric results that depend on countries' characteristics as well as their policy targets (welfare or GDP). Hence, it requires a quantitative model to evaluate the policy impacts of each country.

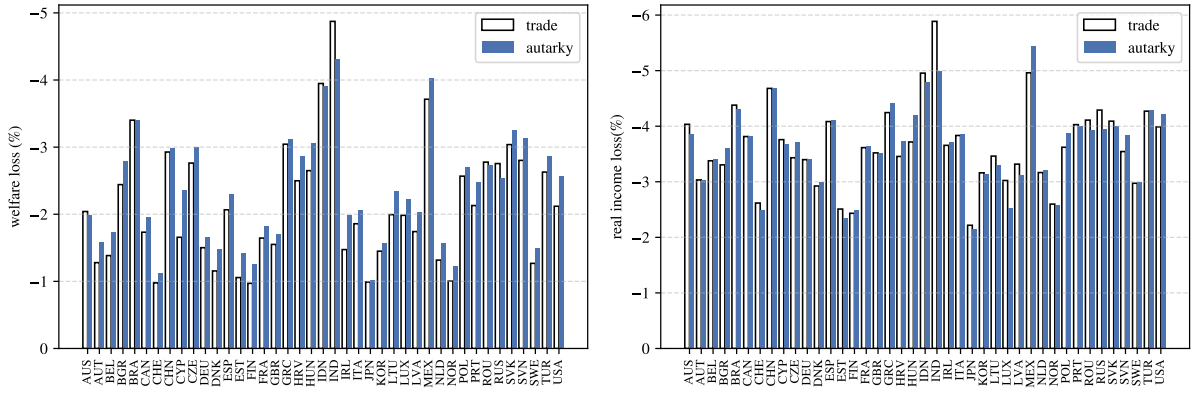


(a) Welfare

(b) Real Income

Figure 3: Welfare and Real-Income Losses Between Trade and Autarky

Second, we further consider how international trade mitigates the pandemic shock. Figure 4 presents the total confirmed cases and total deaths over time with free trade (plotted using dashed line) and in autarky (plotted using solid line). Unlike the results for welfare and real income, trade helps the world to combat a pandemic. For both Figures 4(a) and 4(b), we can observe that there are fewer total confirmed cases and total deaths with trade than in autarky. The number of total deaths under trade is 46.7% of the number under autarky. The intuitions are straightforward: the pandemic shock is perceived differently across different countries and

sectors. As a result, the pandemic also reshapes comparative advantages and patterns of international specialization. Our model shows that a country-sector pair would become relatively more competitive under a pandemic shock if it has greater work-from-home capabilities and less stringent containment measures. International trade would amplify those new competitive edges. Hence, under a pandemic, country-sector pairs with relatively higher work-from-home capability expand, and international trade would amplify the expansions even further. Through trade and international specialization, people in general are less likely to work onsite, as a result, the disease is less likely to be spread via face-to-face interaction in workplaces.

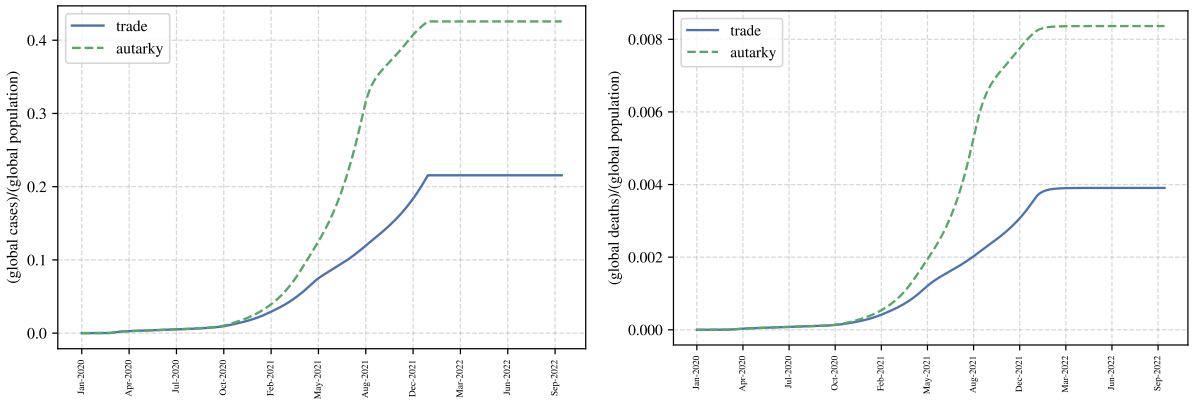


(a) Cumulative Confirmed Cases

(b) Total Deaths

Figure 4: Total Cases and Deaths Between Trade and Autarky Over Time

## 4.2 Optimal Containment Policy

After showing the role of international trade under a pandemic, the next question is about the governments' roles in a pandemic. In this section, we will discuss the results for optimal containment policies.

Before we present the results, we first define the policy tool that each government will utilize. Theoretically, governments of each country could choose a path of containment policies for each period, such that it is welfare maximizing. However, the computational burden for finding entire paths of containment policies for all countries is too heavy. To tackle this problem, we assume governments target effective reproduction numbers. In other words, we assume that each government chooses the maximum of the effective reproductive number to allow, given other countries' effective reproductive numbers. The government would adjust its containment measures accordingly. The equilibrium we find here is essentially a Nash equilibrium because a country's decisions are made given other countries' choices.

Setting a cap on the reproductive number is a reasonable target/representation as it reflects

the speed of disease spread and is the central concern for epidemiologists and doctors who lead government responses. In addition, targeting an effective reproduction number implies that the containment measures should be stringent initially and gradually relaxed over time, which is in line with a pattern found in several recent studies in the macroeconomic literature focusing on the dynamics of optimal policies in closed-economy contexts; see, e.g., Alvarez et al. (2021) and Jones et al. (2021). This is because the fraction of susceptible people in the population, $S_{i,t}/N_i$, diminishes over time; with a fixed target for $R_{e,i,t}$, this implies that containment measures $\eta_{i,t}$ generally decrease over time, provided that the over-time variability of $R_{0,i,t}$ is modest.

#### 4.2.1 Procedure for Computing Optimal Containment Policy

Given that the maximum effective reproductive number is the policy target, we now describe the procedure on how to calculate the optimal policies. Specifically, we will implement the computations in two steps: computing the global uniform policies first and then individual responses later. Solving in two steps makes it feasible to derive the optimal policy by reducing the computational burden.

In the first step, we consider a simpler problem in which a global social planner decides an effective reproduction number $R_e^*$ that applies to all countries such that the global welfare is maximized. Suppose a global social planner decides on an effective reproduction number $R_e^*$ and all countries set up their containment policies $\widetilde{\eta}_{i,t}$ to match $R_e^*$, whenever possible. Namely, for each country $i$, $\{\widetilde{\eta}_{i,t}\}_{t=t_i^*}^{730}$ satisfy

$$R_{e,i,t} = (1-\widetilde{\eta}_{i,t})\left[\pi_i^I + \pi_i^L \sum_{j=1}^{J}(1-\mu_i^j)\ell_{i,t}^j\right] \times 18 \times \frac{S_{i,t}}{N_i} \leq R_e^*, \tag{12}$$

where the equality holds if a positive solution of $\widetilde{\eta}_{i,t}$ exists; otherwise $\widetilde{\eta}_{i,t} = 0$ and the inequality holds. Also, $\widetilde{\eta}_{i,t} = \eta_{i,t}$ for $t < t_i^*$,[5] and $\widetilde{\eta}_{i,t} = 0$ for $t > 730$. The goal of the social planner is to maximize long-run global welfare specified in (10).

Given that $R_e^*$ set by the global planner has been calculated in the first step, we then explore each country's optimal policy in the second step. In particular, the information from the previous step is useful for our algorithm of finding a Nash equilibrium of optimal national policies. Moreover, the effective reproduction number under which the highest welfare for each country is attained is rather close to $R_e^*$. Thus, these numbers are chosen as the initial guess for the iterations for finding a Nash equilibrium, i.e., a fixed point of best responses (optimal national policies). Along with other information from the previous subsection, this suggests that the op-

[5]Note that it is possible that for those days between January 1, 2020 and the onset of the disease evolution, a country may already adopt some containment measures such as border control.

timal $R^*_{e,i}$ for each national planner is likely to be found in the neighborhood of the initial guess. Thus, in our grid search, the grids are much denser in that neighborhood and sparser far away from it. This substantially eases the computational burden. Still, the grid search covers the entire range from a total lock-down to a laissez-faire policy.

Notice that to compare with optimal policies, we compute a long-run baseline case in which countries are assumed to keep doing what they have been doing. That is, their policies from November 17, 2020, onward are projected to entail their realized averages of $R_{e,i,t}$ for the period from the onset of the outbreak $t^*_i$ to November 16, 2020. Their actual policies up to November 16 are used in simulating the baseline.

### 4.2.2 Characterization of the Optimal Policies

Following the algorithms described in the previous section, we present the results. Figure 5 shows the optimal $R^*_{e,i}$ compared with the current average effective reproduction number $\bar{R}_{e,i}$, defined as the over-time average of realized $\{R_{e,i,t}\}$. As before, countries are listed on the x-axis and effective reproduction numbers are on the y-axis, and the shorter the bar, the lower the target of the effective reproduction number.

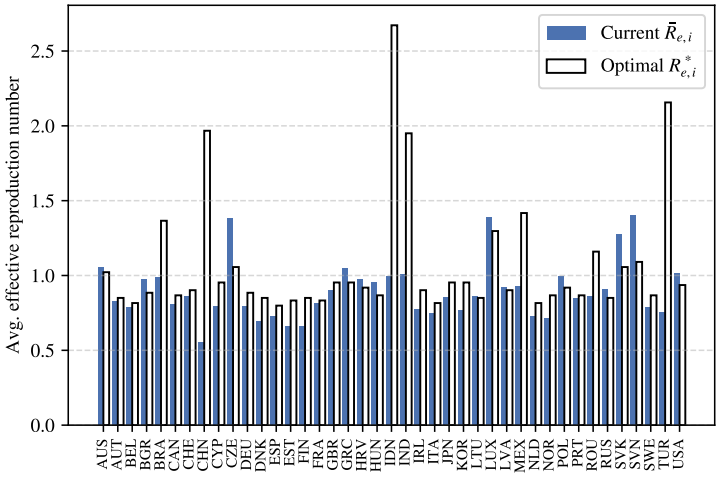


Figure 5: Current Effective Reproduction Number $\bar{R}_{e,i}$ and Optimal Effective Reproduction Number $R^*_{e,i}$

Several observations are in order. First, although most of the $R^*_{e,i}$'s are less than their current corresponding average effective reproduction numbers, there are several countries whose optimal policies are higher than the currently adopted policy. These results imply that although for most countries it is better to adopt more stringent policies, there are countries that would be better off if the containment policies could be eased. Second, most of the optimal policies are targeting an effective reproduction number that is less than (or close to) 1, meaning that it is better

to target the policy that does not allow the pandemic to spread. However, there exist countries, such as BRA, CHN, IDN, IND, MEX, ROU and TUR, which would be better off if the containment policies were largely relaxed. Third, the estimated optimal containment policies should be interpreted as the lower bound of the extent of the optimal stringency, as we intentionally leave out the psychological cost of mortality. Once this cost is incorporated, then those that should tighten up should definitely tighten up even more, whereas the conclusion for those that need to relax may become ambiguous.

The next question is what are the driving forces behind these asymmetric results. Figure 6 shows the intuitions. For all the countries, we observe that the Nash responses can be categorized into two patterns. Hereafter, we demonstrate these two patterns using two countries: the U.S. and India. The results are presented in Figure 6. Figure 6(a) shows how the welfare in the U.S. would change if the global uniform target of the effective reproduction number changes, and Figure 6(b) shows the results for India.

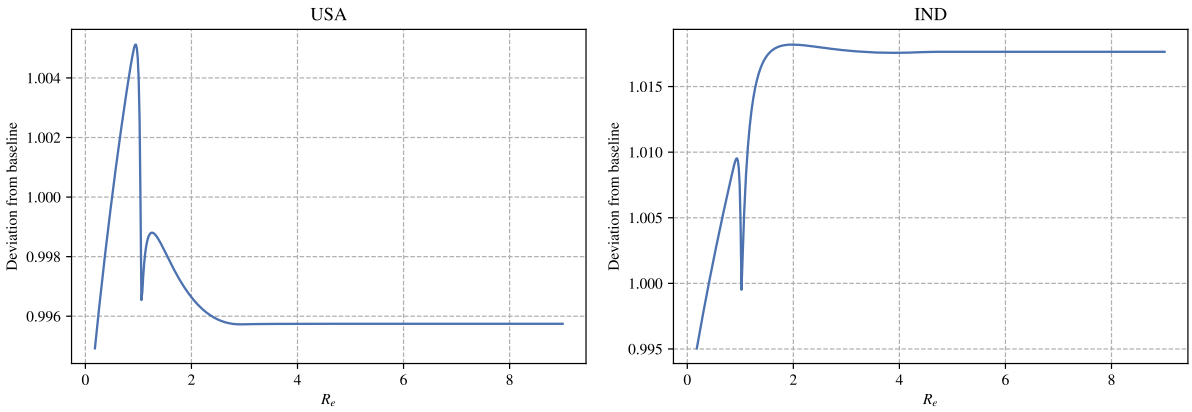


Figure 6: Welfare of Individual Countries across Global Uniform $R_e$

Several observations are also presented in order. First, on both graphs, we observe that there are two hump shapes: the containment policies corresponding to the first hump shape are relatively stricter (for most countries, the peak of the first hump shape occurs when the effective reproduction number is below 1) than those of the second hump shape. Second, the mechanisms that govern the first hump shape are similar for the U.S. and India, but the mechanisms for the right hump shape differ. From the second hump shape, we see the U.S. does not gain much welfare when the containment policies are further relaxed, but India receives higher welfare when the laissez-faire policy is adopted. Third, the first hump shape occurs when the effective reproduction number is relatively small and demonstrates the trade-off between lives and economy. Its peak (the local maximum) indicates the sub-optimal extent of restriction stringency that allows some economic activities while preventing the disease from spreading. Fourth, different patterns of the second hump shape imply that there is a large heterogeneity across countries.

For countries having high $R_0$ or low WFH capacities, it is too costly to adopt a very strict containment policy. As a result, the laissez-faire policy will be preferred. This result is not trivial considering this is an impact on long-run welfare from the shocks in a two-year plus period.[6]

Hence, we can conclude that in an international trade model with a pandemic, lives and economy are the first order priority to be considered. However, several other factors such as WFH abilities as well as dependence on international trade would also affect the results. It is not surprising that in a pandemic affecting all countries that there is no easy solution or guidelines for everyone to follow.

#### 4.2.3 The Role of International Trade under Optimal Containment Policy

After demonstrating the optimal containment policies, we now discuss how international trade plays an important role. Specifically, we examine how the optimal policies differ when countries switch to autarky. Note that this exercise actually computes the optimal policies by simulating the counterfactual case in which each country is in the closed economy.

Figure 7 shows the change in optimal $R^*_{e,i}$ when the economy switches from an open economy to a closed economy. We present the different countries on the x-axis and the differences in optimal policies between autarky and trade on the y-axis. These numbers indicate whether a country would implement more or less stringent containment measures in autarky. A positive number implies that a government would implement less stringent containment policies under autarky. The results are mixed. Due to complex trade linkages, there is no unanimous sign of the deviation. However, optimal $R^*_{e,i}$ under trade is lower than that of under autarky for most countries (35 out of 41). These indicate that optimal containment policies are generally tighter with trade than in autarky. This is because trade generally acts as a buffer from pandemic shocks and provides the governments more headroom to implement policies to combat the pandemic. Thus, with trade, national planners suffer from losses in production and income to a lesser extent, thereby allowing them to adopt stricter restrictions that would save more lives, which in turn would benefit the economy in a longer term.

To further examine the magnitudes of the differences, we calculate the relative difference in absolute value for each country as follows:

$$\frac{|\text{Welfare Improvement under Autarky - Welfare Improvement under Trade}|}{\text{Welfare Improvement under Trade}}.$$

The average relative difference is 0.45 (which is translated into 0.15% relative to the welfare improvement under trade). The corresponding standard deviation for the relative difference is

[6]We let the simulation run about 200 more days after an effective vaccine is available so that epidemiological evolution gradually subsides such that $I_{i,t} \to 0$ for all countries.

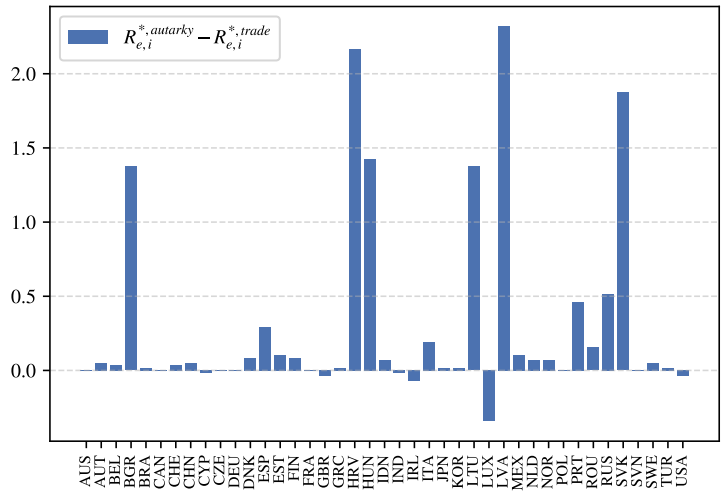


Figure 7: Comparison of Optimal Policies between Trade and Autarky

0.38, indicating large variations across countries. Thus, incorporating trade is both qualitatively and quantitatively important in determining the optimal policy.

In sum, international trade plays a key role in combating a pandemic. Not only it does help to flatten the curve and save many more lives but it also acts as a buffer to welfare losses from the pandemic. When a global pandemic takes place such as COVID-19, countries could help each other out by sourcing higher-risk sectors from countries that are better shielded from the pandemic.

### 4.3 Limitations

So far, we have shown the role of international trade under the COVID-19 pandemic, the optimal policy of each country, and how trade helps when a country considers its best responses. In this subsection, we revisit these assumptions and parameters we impose in the model and show whether our results are sensitive to specific settings.

First, it has been shown in the literature that the role of input-output linkages is important in a trade model. For our baseline model, we abstract from input-output linkages in order to highlight the importance of international trade. However, it is crucial to understand whether the input-output linkages would change our results. A version of the model with full-fledged input-output linkages is presented in Appendix B. We simulate the model with I-O linkages, and we compare economic and health outcomes under trade and under autarky. We show the welfare and GDP losses between trade and autarky with I-O linkages in Figure 8, and then we demonstrate the total confirmed cases and total deaths over time with I-O linkages in Figure 9.

In Figure 8(a) and Figure 8(b), we can observe that results follow qualitatively similar patterns as in the case without IO linkages. The effects from trade are mixed, but largely trade

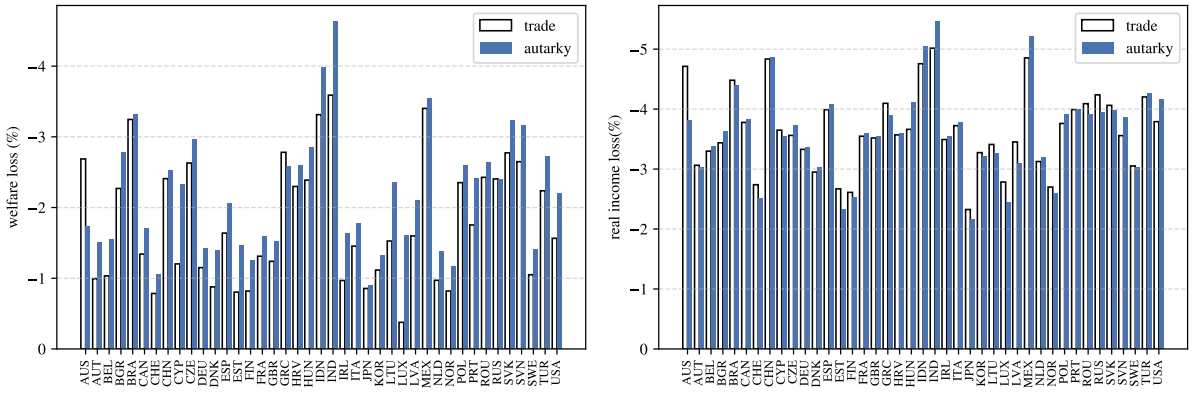


(a) Welfare (b) Real Income

Figure 8: Welfare and Real-Income Losses Between Trade and Autarky with I-O Linkages

improves both welfare and GDP, while the effects for GDP are much smaller than the effects for welfare. A noticeable difference is that the differences between trade and autarky are larger in the case with I-O linkages.

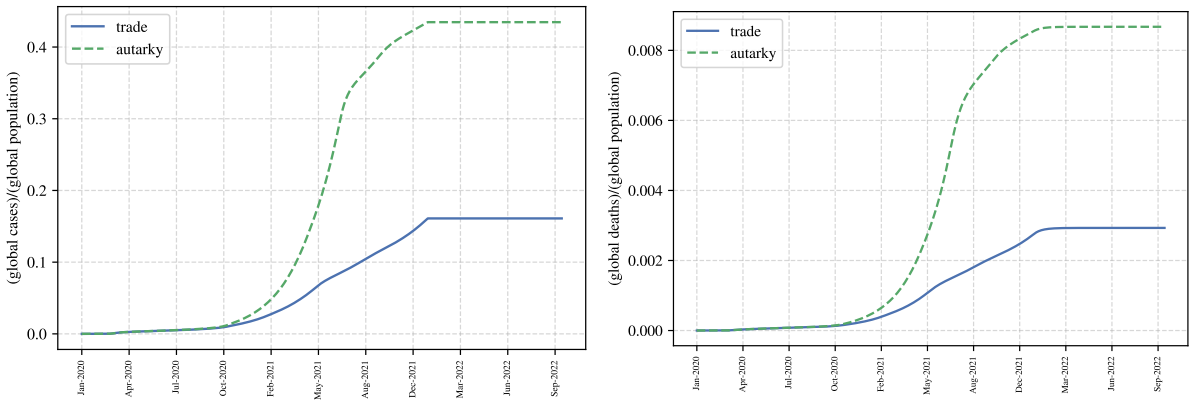


(a) Cumulative Confirmed Cases (b) Total Deaths

Figure 9: Total Cases and Deaths Between Trade and Autarky Over Time with I-O

As for the results on total confirmed cases and total deaths, similar patterns can be observed in Figure 9(a) and Figure 9(b). The flattening-the-curve effect is preserved with the presence of I-O linkages, and the number of total deaths under trade is 39% of the number under autarky. In comparison to our benchmark case, more deaths are averted. This is mainly due to the fact that input-output linkages further strengthen the new comparative advantages and international specialization, and even more people can work from home safely. This result suggests that our qualitative results remain robust with the addition of input-output linkages.

Next, we examine whether our results are sensitive to the specifications of epidemiological evolution. Notice that we calibrate the results until November 16, 2020, in order to be abstract

from the effects of vaccinations and various variants of COVID-19. We simulate our model under different epidemiological parameter values, and we check whether our results are robust for various specification.

All the results are presented in Appendix Table 1. We consider five different scenarios: (1) case fatality rate = 1%, (2) case fatality rate = 3%, (3) $R_0 = 0.9 * R_0^{benchmark}$, (4) $R_0 = 1.1 * R_0^{benchmark}$, and (5) the pandemic ends in 4 years. In order to demonstrate how sensitive our results are, especially on the role of international trade, we present the percentage change of trade-to-autarky outcomes relative to benchmark of each scenario. In Appendix Table 1, we can observe that most of the magnitudes and signs are similar to the benchmark, and this implies that our main take-away will not change if a different pandemic is considered. Although we do observe that results are more sensitive to the case of the basic reproduction number $R_0$, the driving forces behind our model seem to remain unchanged.

In sum, we have shown that our implications are robust. Even though we did not model vaccinations, COVID-19 variants, or input-output linkages, our quantitative model suggests that international trade plays an important role in the COVID-19 pandemic. Trade fosters new comparative advantages under the pandemics shocks and moves people away from sectors that are not shielded well from COVID-19. As a result, trade would make it easier for governments around the world to try more stringent policies to combat the pandemic and flatten the curve.

## 5 Conclusion

The novelty of this work is to use effective reproduction numbers as policy targets to reduce the space of candidate policies in a model with rich cross-sectional links across countries and sectors and with these links interacting with disease dynamics. Our quantitative analyses prove to be informative; the takeaway messages are as follows.

First, we demonstrate the importance of international trade during the pandemic. We find that trade works as a buffer to the pandemic shocks. Welfare loss and total deaths are reduced under international trade. In addition, trade also helps to flatten the curve. Second, we use a novel approach to solve for the optimal containment policies for 41 countries. In terms of optimal national policies, a majority of countries need to tighten up, whereas only a handful of countries need to relax. Psychological costs of mortality are intentionally left out of the model. When such costs are incorporated, those countries that should tighten up should tighten up even more, and the welfare implications are even larger.

## References


Acemoglu, D., Chernozhukov, V., Werning, I., and Whinston, M. D. (2021). Optimal targeted lockdowns in a multigroup sir model. *American Economic Review: Insights*, 3(4):487–502.

Alvarez, F., Argente, D., and Lippi, F. (2021). A Simple Planning Problem for COVID-19 Lockdown, Testing, and Tracing. *American Economic Review: Insights*, 3(3):367–82.

Antrás, P., Redding, S. J., and Rossi-Hansberg, E. (2020). Globalization and Pandemics. NBER Working Paper 27840.

Argente, D., Hsieh, C.-T., and Lee, M. (2021). The Cost of Privacy: Welfare Effects of the Disclosure of COVID-19 Cases. *The Review of Economics and Statistics*, pages 1–29.

Atkeson, A. (2020). On using SIR Models to Model Disease Scenarios for COVID-19. *Quarterly Review*, 41(1):1–35. Federal Reserve Bank of Minneapolis.

Atkeson, A. G., Kopecky, K., and Zha, T. (2021). Behavior and the Transmission of COVID-19. *AEA Papers and Proceedings*, 111:356–60.

Bonadio, B., Huo, Z., Levchenko, A. A., and Pandalai-Nayar, N. (2021). Global Supply Chains in the Pandemic. *Journal of International Economics*, 133:103534.

Budish, E. B. (2020). Maximize utility subject to $R \leq 1$: A Simple Price-theory Approach to COVID-19 Lockdown and Reopening Policy. NBER Working Paper 28093.

Caliendo, L. and Parro, F. (2015). Estimates of the Trade and Welfare Effects of NAFTA. *The Review of Economic Studies*, 82(1):1–44.

Chen, J., Chen, W., Liu, E., Luo, J., and Song, Z. M. (2020). The Economic Impact of COVID-19 in China: Evidence from City-to-City Truck Flows. Working Paper, Princeton University.

Dingel, J. I. and Neiman, B. (2020). How Many Jobs Can be Done at Home? *Journal of Public Economics*, 189:104235.

Dong, E., Du, H., and Gardner, L. (2020). An Interactive Web-based Dashboard to Track COVID-19 in Real Time. *The Lancet Infectious Diseases*, 20(5):533–534.

Eaton, J. and Kortum, S. (2002). Technology, Geography, and Trade. *Econometrica*, pages 1741–1779.

Eichenbaum, M. S., Rebelo, S., and Trabandt, M. (2021). The Macroeconomics of Epidemics. *The Review of Financial Studies*, 34(11):5149–5187.

Eppinger, P., Felbermayr, G., Krebs, O., and Kukharskyy, B. (2020). COVID-19 Shocking Global Value Chains. Cesifo working paper.

Fajgelbaum, P. D., Khandelwal, A., Kim, W., Mantovani, C., and Schaal, E. (2021). Optimal Lockdown in a Commuting Network. *American Economic Review: Insights*, 3(4):503–22.

Farboodi, M., Jarosch, G., and Shimer, R. (2021). Internal and External Effects of Social Distancing in a Pandemic. *Journal of Economic Theory*, 196:105293.

Fieler, A. C. (2011). Nonhomotheticity and Bilateral Trade: Evidence and a Quantitative Explanation. *Econometrica*, 79(4):1069–1101.

Hale, T., Angrist, N., Cameron-Blake, E., Hallas, L., Kira, B., Majumdar, S., Petherick, A., Phillips, T., Tatlow, H., and Webster, S. (2020). Oxford COVID-19 Government Response Tracker. *Blavatnik School of Government*.

Head, K. and Mayer, T. (2014). Gravity Equations: Workhorse, Toolkit, and Cookbook. In *Handbook of International Economics*, volume 4, pages 131–195. Elsevier.

Jones, C., Philippon, T., and Venkateswaran, V. (2021). Optimal Mitigation Policies in a Pandemic: Social Distancing and Working from Home. *The Review of Financial Studies*, 34(11):5188–5223.

Kermack, W. O., McKendrick, A. G., and Walker, G. T. (1927). A Contribution to the Mathematical Theory of Epidemics. *Proceedings of the Royal Society of London. Series A, Containing Papers of a Mathematical and Physical Character*, 115(772):700–721.

Krueger, D., Uhlig, H., and Xie, T. (2020). Macroeconomic Dynamics and Reallocation in an Epidemic. NBER Working Paper 27047.

Low, H. and Pistaferri, L. (2015). Disability Insurance and the Dynamics of the Incentive Insurance Trade-Off. *American Economic Review*, 105(10):2986–3029.

Mayer, T. and Zignago, S. (2011). Notes on CEPII's Distances Measures: The GeoDist database.

Piguillem, F. and Shi, L. (2020). Optimal COVID-19 Quarantine and Testing Policies. EIEF Working Papers Series 2004, Einaudi Institute for Economics and Finance (EIEF).

Ravikumar, B., Santacreu, A. M., and Sposi, M. (2019). Capital Accumulation and Dynamic Gains from Trade. *Journal of International Economics*, 119:93–110.

Simonovska, I. and Waugh, M. E. (2014). The Elasticity of Trade: Estimates and Evidence. *Journal of International Economics*, 92(1):34 – 50.

The Lancet Microbe (2021). COVID-19 Vaccines: the Pandemic will not End Overnight. *The Lancet Microbe*, 2(1):e1.

Timmer, M. P., Dietzenbacher, E., Los, B., Stehrer, R., and De Vries, G. J. (2015). An Illustrated User Guide to the World Input-Output Database: the Case of Global Automotive Production. *Review of International Economics*, 23(3):575–605.

WHO (2020). Coronavirus disease 2019 (covid-19): situation report, 46.

# Appendix

## A Quantification

Our model consists of two sets of parameters: economic and epidemiological. We describe how they are calibrated in order.

### A.1 Economic Parameters

#### A.1.1 Risk aversion and time preference

For our quantitative analyses, we set the per-period utility as

$$u(q) = \frac{(q+1)^{1-\sigma} - 1}{1-\sigma}.$$

We choose this functional form for three reasons. First, this specification is similar to the CRRA (constant relative risk aversion) utility if the term $q + 1$ is replaced with $q$. Thus, it is approximately CRRA when $q$ is large; the parameter $\sigma$ measures the degree of relative risk aversion. Second, $u(0) = 0$, which satisfies our requirement that psychological costs be left out of the model; note that the exact CRRA utility entails $\lim_{q\to 0} u(q) \to -\infty$ when $\sigma \geq 1$ and is therefore not implementable. Third, $\sigma = 0$ corresponds to the risk-neutral case. Following Low and Pistaferri (2015), the relative risk aversion $\sigma$ is set to 1.5. Following Farboodi et al. (2021), we set the annual discount rate as $0.95$; as daily data is used, $\rho = 0.95^{\frac{1}{365}} \approx 0.99986$.

#### A.1.2 WIOD

Our main data source is the World Input-Output Database (WIOD), which contains information on bilateral trade for intermediates and for final goods for 43 countries and 56 industries. The country of Malta is dropped as it is not included in the data on containment policy from the Oxford COVID-19 Government Response Tracker. Table 2 lists the 41 countries in the data. We use the data from the year 2014, the latest available year in the WIOD, and aggregate 56 industries into 6 sectors. See Table 3 for the list of industries and sectors. Two industries are left out of our aggregation (activities of households as employers and activities of extraterritorial organizations and bodies) since there is no corresponding work-from-home capability in Dingel and Neiman (2020).

Under the Social Economic Account, the database also provides information on total labor compensation and the total number of persons engaged for each industry; these allow for calculating country-specific wages. See Timmer et al. (2015).

Also, from the WIOD, we obtain data on gross production across countries and sectors as well as each sector $j$'s use of intermediates across countries and sectors. The data also include sectoral final consumption across countries. For the our model with I-O linkages, we can compute the shares of intermediate use $\gamma_i^{j,l}$ as the shares of total intermediate use by sector $j$ on goods from sector $l$. The shares of intermediate in gross output, $1-\beta_i^j$, is calculated by the total intermediate use divided by the gross production. The final consumption shares $\alpha_i^j$ are computed by total sector-$j$ final consumption divided by the total final consumption.

### A.1.3 Estimation of productivity parameters $\{T_i^j\}$ and trade costs $\{\tau_{i,n}^j\}$

Given the data on trade shares and geography from the WIOD and Centre d'Études Prospectives et d'Informations Internationales (CEPII), the model's gravity equations and hence trade costs $\{\tau_{i,n}^j\}$ can be estimated. Following Simonovska and Waugh (2014), we set the value of trade elasticity $\theta = 4$. Given trade elasticity, estimated trade costs, various share parameters $\{\alpha_i^j, \beta_i^j, \gamma_i^{j,l}\}$, and data on wages obtained from the Social Economic Account in the WIOD, the productivity parameters $\{T_i^j\}$ can then be backed out using the model structure. We describe the estimation of trade costs and productivity parameters in order.

**Gravity Equation** We use a standard approach in estimating productivity parameters $\{T_i^j\}$ and trade costs $\{\tau_{i,n}^j\}$. Start with the model's gravity equation:

$$X_{i,n}^j = \frac{T_i^j (c_i^j \tau_i^j)^{-\theta}}{\Phi_n^j} X_n^j.$$

Taking the logarithm of both sides, we have

$$\ln X_{i,n}^j = \ln[T_i^j (c_i^j)^{-\theta}] + \ln[(\tau_{i,n}^j)^{-\theta}] + \ln[X_n^j (\Phi_n^j)^{-1}].$$

Assume that trade costs take the functional form below,

$$-\theta \ln \tau_{i,n}^j = \nu_0^j \ln(dist_{i,n}) + \nu_2^j contig_{i,n} + \nu_3^j comlang_{i,n} + \nu_4^j colony_{i,n},$$

where $dist_{i,n}$ is the distance between $i$ and $n$ in thousands of kilometers, and $contig_{i,n}$ equals one if countries $i$ and $n$ share a border. Analogously, $comlang_{i,n}$ and $colony_{i,n}$ indicate whether two countries share the same language and colonial historical links. These variables are obtained from the GeoDist database from the Centre d'Etudes Prospectives et d'Informations Internationales (CEPII) (see Mayer and Zignago (2011)). Thus, the empirical specification is

$$\ln X_{i,n}^j = \nu_0^j \ln(dist_{i,n}) + \nu_2^j contig_{i,n} + \nu_3^j comlang_{i,n} + \nu_4^j colony_{i,n} + D_i^{j,exp} + D_n^{j,imp} + \varepsilon_{i,n}^j$$

Following Head and Mayer (2014), we apply OLS to estimate the fixed effects model to obtain estimates of $\{\nu^j, D_i^{j,exp}\}$.

**Uncovering Productivity Parameters** We follow the trade literature, in particular Simonovska and Waugh (2014), and set $\theta = 4$. Trade costs $\{\tau_{i,n}^j\}$ can be calculated using the estimated coefficients:

$$\hat{\tau}_{i,n}^j = \exp\left(\frac{\hat{\nu}_0^j \ln(dist_{i,n}) + \hat{\nu}_2^j contig_{i,n} + \hat{\nu}_3^j comlang_{i,n} + \hat{\nu}_4^j colony_{i,n}}{-\theta}\right).$$

Then, we use the estimated exporter dummies and data on wages to obtain $T_i^j$ by the following procedure. First, observe that

$$\hat{T}_i^j = \exp(\hat{D}_i^{j,exp}) \times (c_i^j)^\theta,$$

where $c_i^j$ is the unit cost of production. In this section, we describe the scenario with I-O linkages, where $c_i^j = w_i^{\beta_i^j}(P_i^{M,j})^{1-\beta_i^j}$, and the benchmark case (absence of I-O linkages) is a degenerate version of the with I-O linkages cases. As mentioned in Appendix A.1.2, wages $w_i$ are observed from the Social Economic Account in the WIOD. Hence,

$$\hat{T}_i^j = \exp(\hat{D}_i^{j,exp}) \times [w_{i,data}^{\beta_i^j}(\hat{P}_i^{M,j})^{1-\beta_i^j}]^\theta \tag{13}$$

$$\hat{P}_i^{M,j} = \prod_{l=1}^{J}(\hat{P}_i^l)^{\gamma_i^{j,l}} \tag{14}$$

$$\hat{P}_i^j = \Gamma\left(\frac{\theta - 1 + \kappa}{\theta}\right)\left[\sum_{k=1}^{K}\hat{T}_k^j[w_{i,data}^{\beta_i^j}(\hat{P}_i^{M,j})^{1-\beta_i^j}\hat{\tau}_{i,k}^j]^{-\theta}\right]^{-\frac{1}{\theta}}. \tag{15}$$

The following procedure is used to solve for $\{T_i^j\}$, as in Fieler (2011) and Ravikumar et al. (2019). Let $r$ index the rounds of iterations, and start with an initial guess of $\{\hat{P}_i^{M,j}(0)\}$.

1. Update productivity: $\hat{T}_i^j(r) = \exp(\hat{D}_i^{j,exp}) \times [w_{i,data}^{\beta_i^j}\hat{P}_i^{M,j}(r)^{1-\beta_i^j}]^\theta$.
2. Update sectoral price indices: $\hat{P}_i^j(r) = \Gamma\left(\frac{\theta - 1 + \kappa}{\theta}\right)\left[\sum_{k=1}^{K}\hat{T}_k^j(r)(w_{i,data}^{\beta_i^j}\hat{P}_i^{M,j}(r)^{1-\beta_i^j}\hat{\tau}_{i,k}^j)^{-\theta}\right]^{-\frac{1}{\theta}}$.
3. Update the price indices of the intermediate-input bundle: $\hat{P}_i^{M,j}(r+1) = \prod_{l=1}^{J}[\hat{P}_i^l(r)]^{\gamma_i^{j,l}}$.
4. Stop the iterations if

$$||\hat{P}_i^{M,j}(r+1) - \hat{P}_i^{M,j}(r)|| < tolerance.$$

   Otherwise, go back to Step 1.

5. Take $\hat{T}_i^j(r+1)$ as our new estimates of country-sector-specific productivity parameters.

For the model without input-output linkages, the calibration is the same except that $\beta_i^j = 1$ in (13) and (15) and also (14) is not used.

### A.1.4 Work-from-home capacity

To measure work-from-home capacity by industry, we use the data from Dingel and Neiman (2020), who compute work-from-home capacity by occupation. We use the data aggregated to the 3-digit NAICS and adopt the version in which each occupation's capacity was manually assigned by these authors by inspecting the definitions of the occupations. Our results remain similar when using the other version, which is algorithm based. The data was downloaded from https://github.com/jdingel/DingelNeiman-workathome.

To calculate each WIOD industry's work-from-home capacity, we map each WIOD industry to one or multiple 3-digit NAICS industries according to their definitions. Six WIOD industries map directly into two-digit NAICS, in which cases the 2-digit NAICS work-from-home capacity computed by these authors are used. When a WIOD industry maps into multiple NAICS industries, we proxy the WIOD industry's work-from-home capacities by the average across the corresponding NAICS industries weighted by their industrial employment. The industrial employment data is obtained from the Quarterly Workforce Indicators (QWI) under the LEHD program of the Census Bureau (https://ledextract.ces.census.gov/static/data.html); the fourth quarter of 2014 was used as our WIOD data is for 2014. By-industry and by-state employment data is obtained from QWI, and the industrial employment is the sum across all states. This procedure creates a $\{\mu^j\}$ for WIOD industries.

In our aggregation of WIOD industries into six sectors, the work-from-home capacity for each country-sector pair $\mu_i^j$ is computed as the average of these capacities across industries in that sector, weighted by the industrial employment in that country as obtained from the WIOD data.

### A.1.5 Containment measures

The containment measures $\{\eta_{i,t}\}$ across countries and time are directly obtained from the *Stringency Index* of the Oxford COVID-19 Government Response Tracker (OxCGRT; Hale et al. 2020) at a daily frequency. This index summarizes a government's responses in terms of various closures and containment, including school and workplace closures, stay-at-home requirements, border control, and restrictions on gathering, public events, public transport, and internal movements, as well as public information campaigns.[7]

[7]For more details, see Hale et al. (2020) and https://www.bsg.ox.ac.uk/research/research-projects/coronavirus-government-response-tracker.

## A.2 Epidemiological Parameters

The epidemiological parameters to be calibrated are $\{\pi^r, \pi^d, \delta, \pi_i^I, \pi_i^L, \alpha^I, I_{i,0}\}$. As in Atkeson (2020) and several other macro-SIR models, we set

$$\pi^r + \pi^d = \frac{1}{18}\,, \tag{16}$$

which means that it takes on average 18 days to either recover or die from the infection.

The case fatality rate is set at $\pi^d = 0.016 \times \frac{1}{18}$.[8] Following Alvarez et al. (2021), we set $\delta = 0.05 \times \frac{1}{18}$. As a WHO (2020) COVID-19 Situation Report indicates that asymptotic and mild cases account for about 80% of the infections, we set $\alpha^I = 0.8$.

For our purpose, it is important to quantify infection probabilities $\{\pi_i^I, \pi_i^L\}$, as they are the key parameters underlying the variations in the rate of disease reproduction across countries, besides economic conditions and containment policies. Also, for the epidemiological evolution to commence, an estimate of $I_{i,0}$ is required (as $S_{i,0} = N_i - I_{i,0}$ and $R_{i,0} = D_{i,0} = 0$); $I_{i,0}$ is generally unknown because the society might be unaware of, unprepared for, or on low alert for the disease, so that the number of the first few reported cases may be quite off. To estimate the country-specific infection parameters $\{\pi_i^I, \pi_i^L, I_{i,0}\}$, we will use non-linear least squares to fit the data of total deaths for each country. Note that, however, calculating total deaths in this global economy where countries are interlinked in various ways as explained in the main text is time consuming; hence such estimation is infeasible. In particular, the sectoral employment shares $\{\ell_{i,t}^j\}$ are time varying and determined by the entire vector $\{\pi_i^I, \pi_i^L, I_{i,0}\}_{i=1}^{41}$ for all 41 countries. Thus, the space of candidate estimates is too large to be feasible.

Thus, we adopt a simpler approach to estimate $\{\pi_i^I, \pi_i^L, I_{i,0}\}$ by proxying sectoral employment shares $\{\ell_{i,t}^j\}$ by such shares in the pre-COVID-19 global economy $\{\ell_i^{j,\text{pre}}\}$. Then, the effective reproduction number becomes

$$\begin{aligned} R_{e,i,t} \equiv \frac{T_{i,t}}{I_{i,t}} \times 18 &= (1-\eta_{i,t}) \left[ \pi_i^I + \pi_i^L \times \sum_{j=1}^{J} (1-\mu_i^j) \ell_i^{j,\text{pre}} \right] \times 18 \times \frac{S_{i,t}}{N_i} \\ &\equiv (1-\eta_{i,t}) \times R_{0,i} \times \frac{S_{i,t}}{N_i}. \end{aligned}$$

When the disease dynamics are modified this way, the estimation can be done country by country, and the basic reproduction number $R_{0,i,t}$ also becomes a constant $R_{0,i}$. We first estimate the rates of transmission and initial infections, $\{R_{0,i}, I_{i,0}\}$, simultaneously, and then back out infection probabilities $\{\pi_i^I, \pi_i^L\}$.

[8] This number is estimated as a case fatality rate. This choice of mortality rate is consistent with our estimation of key parameters using official data on the number of cases as described below.

Let $t_i^*$ denote the first date on which country $i$'s number of total confirmed cases exceeds 50, and assume that the previous day $t_i^* - 1$ is when $I_{i,0}$ is applied. Let $T$ be the latest available data date of the Stringency Index for all countries in our sample (November 16, 2020). For each country $i$, we estimate the following equation using nonlinear least squares:

$$(\hat{R}_{0,i}, \hat{I}_{i,0}) = \text{argmin} \sum_{t=t_i^*}^{T} \left[C_{i,t,data} - C_{i,t}(R_{0,i}, I_{i,0}; \boldsymbol{\eta}_{i,T})\right]^2,$$

where $\boldsymbol{\eta}_{i,T}$ is the full history of $\eta_{i,t}$ up to date $T$, $C_{i,t}$ is the number of total deaths at date $t$ from the model, and $C_{i,t,data}$ is the number of total deaths downloaded from the Humanitarian Data Exchange website.[9] This website compiles data from the Johns Hopkins University Center for Systems Science and Engineering (JHU CCSE), which documents for COVID-19 the numbers of total cases, total deaths, and daily confirmed cases for more than 200 countries and regions.

Borrowing from the results in Eichenbaum et al. (2021), we assume that $2/3$ of the infections come from general activities. With estimated $\{\hat{R}_{0,i}\}$, $\{\pi_i^I, \pi_i^L\}$ can then be solved from

$$\pi_i^I + \pi_i^L \sum_{j=1}^{J} (1 - \mu_i^j) \ell_i^{j,\text{pre}} = \frac{\hat{R}_{0,i}}{18}, \tag{17}$$

$$\frac{\pi_i^I}{\pi_i^I + \pi_i^L \sum_{j=1}^{J} (1 - \mu_i^j) \ell_i^{j,\text{pre}}} = \frac{2}{3}. \tag{18}$$

Note that in our quantitative analyses, the disease dynamics and, in particular, the effective reproduction number $R_{e,i,t}$ are still generated from the full model.

# B A Model with Input-Output linkages

In this section, we briefly describe a model with input-output linkages. The model follows a roundabout production structure as in Caliendo and Parro (2015).

## B.1 Production

Labor is the fundamental input for production, and the production in each sector potentially uses intermediate inputs from all sectors. Let $M_{i,t}^j(\omega)$ denote the use of the composite intermediate goods by the firms producing variety $\omega$ in sector $j$ and country $i$; it is made of a Cobb-Douglas composite:

$$M_{i,t}^j = \prod_{l=1}^{j} (q_{i,t}^{M,l})^{\gamma_i^{j,l}}, \tag{19}$$

[9] Novel Coronavirus (COVID-19) Cases Data https://data.humdata.org/dataset/novel-coronavirus-2019-ncov-cases.

where the sectoral good $q_{i,t}^{M,l}$ is made by the same CES aggregator across varieties as in (1) with the inputs being $q_{i,t}^{M,j}(.)$. Note that each sector $j$'s intermediate composite's expenditure share on sector $l$'s good, $\gamma_i^{j,l}$, is country specific.

Denote a country-sector-time-specific pandemic shock parameter on the production function by $B_{i,t}^j$. The production function of a variety $\omega$ in sector $j$ and country $i$ is given by

$$y_{i,t}^j(\omega) = \frac{z_i^j(\omega)\left[B_{i,t}^j L_{i,t}^j(\omega)\right]^{\beta_i^j} M_{i,t}^j(\omega)^{1-\beta_i^j}}{(\beta_i^j)^{\beta_i^j}(1-\beta_i^j)^{1-\beta_i^j}}, \tag{20}$$

where $L_{i,t}^j(\omega)$ is the labor hired for this variety, $\beta_i^j$ is the labor share, and the Hicks-neutral productivity $z_i^j(\omega)$ is drawn *i.i.d.* from a Fréchet distribution: $\Pr(x < z) = \exp(-T_i^j z^{-\theta})$.

The unit cost of delivering a good from country $i$ to country $n$ is $c_{i,t}^j \tau_{i,n}^j / z_{i,t}^j(\omega)$, and

$$c_{i,t}^j = \left(\frac{w_{i,t}}{B_{i,t}^j}\right)^{\beta_i^j} (P_{i,t}^{M,j})^{1-\beta_i^j},$$

where $w_{i,t}$ and $P_{i,t}^{M,j}$ are country $i$'s wages and its sector $j$'s price for obtaining the intermediate input bundle specified in (19), respectively. Each country $n$ buys from the cheapest source: $p_{n,t}^j(\omega) = \min_i \left\{c_{i,t}^j \tau_{i,n}^j / z_{i,t}^j(\omega)\right\}$. Standard derivations yield the price indices:

$$P_{i,t}^j = \left(\int_0^1 p_{i,t}^j(\omega)^{1-\kappa}\right)^{\frac{1}{1-\kappa}}, \quad P_{i,t}^{M,j} = \prod_{l=1}^J \left[P_{i,t}^l\right]^{\gamma_i^{j,l}}, \quad P_{i,t} = \prod_{j=1}^J \left[P_{i,t}^j\right]^{\alpha_i^j}. \tag{21}$$

### B.2 Price Indices and Trade Shares

Assuming $\kappa < \theta + 1$, the price index of a sectoral good with input-output linkages is given by

$$P_{n,t}^j = \zeta \left(\sum_{k=1}^K T_k^j \left[\left(w_{k,t}/B_{k,t}^j\right)^{\beta_k^j} \left(P_{k,t}^{M,j}\right)^{1-\beta_k^j} \tau_{k,n}^j\right]^{-\theta}\right)^{-\frac{1}{\theta}}, \tag{22}$$

where $\zeta \equiv \left[\Gamma\left(\frac{\theta+1-\kappa}{\theta}\right)\right]^{1/(1-\kappa)}$, and the expenditure share of sector-$j$ goods that country $n$ purchases from country $i$ is given by

$$\pi_{i,n,t}^j = \frac{T_i^j \left[\left(w_{i,t}/B_{i,t}^j\right)^{\beta_i^j} \left(P_{i,t}^{M,j}\right)^{1-\beta_i^j} \tau_{i,n}^j\right]^{-\theta}}{\sum_{k=1}^K T_k^j \left[\left(w_{k,t}/B_{k,t}^j\right)^{\beta_k^j} \left(P_{k,t}^{M,j}\right)^{1-\beta_k^j} \tau_{k,n}^j\right]^{-\theta}}. \tag{23}$$

### B.3 Market Clearing Conditions

With input-output linkages, the market clearing condition for labor becomes

$$w_{i,t} L_{i,t} = \sum_{j=1}^J \beta_i^j R_{i,t}^j = \sum_{j=1}^J \sum_{n=1}^K \beta_i^j \pi_{i,n,t}^j X_{n,t}^j. \tag{24}$$

And the goods market clearing condition follows

$$X_{i,t}^{j} = \underbrace{\underbrace{\alpha_i^j w_{i,t} L_{i,t}}_{\text{consumption}} + \sum_{l=1}^{J} \underbrace{\gamma_i^{l,j}(1-\beta_i^l) \sum_{n=1}^{K} \pi_{i,n,t}^{l} X_{n,t}^{l}}_{\text{as intermediate for sector } l}}_{\text{total demand}} . \tag{25}$$

Sectoral employment shares are computed by $\ell_{i,t}^{j} = \beta_i^j R_{i,t}^{j} / \sum_{l=1}^{J} \beta_i^l R_{i,t}^{l}$.

# C Additional Tables

We present additional tables here for the reason of saving space in the main body. First, we present the sensitivity analysis. We consider five different scenarios: (1) case fatality rate = 1%, (2) case fatality rate = 3%, (3) $R_0 = 0.9 * R_0^{benchmark}$, (4) $R_0 = 1.1 * R_0^{benchmark}$, and (5) the pandemic ends in 4 years. We present the percentage change of trade-to-autarky outcomes relative to benchmark of each scenario. Second, we present the country list. Last, we present the WIOD sector list.

Table 1: Sensitivity Analysis

| | Death Rate = 1% | | Death Rate = 3% | | $R_0 = 0.9 * R_0^{old}$ | | $R_0 = 1.1 * R_0^{old}$ | | $t^* = 1440$ days | |
|---|---|---|---|---|---|---|---|---|---|---|
| | Welfare | Death | Welfare | Death | Welfare | Death | Welfare | Death | Welfare | Death |
| World | 2.71% | -3.81% | -5.10% | 3.61% | 2.62% | 15.34% | 8.57% | 107.72% | 10.43% | 105.70% |
| | | | | | | | | | | |
| AUS | -9.21% | 7.50% | 19.34% | -5.93% | -28.31% | -35.34% | -26.83% | -82.00% | -29.74% | -81.56% |
| AUT | -2.38% | 0.20% | 5.43% | -0.14% | -3.44% | -50.79% | 43.14% | 93.34% | -3.67% | 71.54% |
| BEL | -2.52% | -0.10% | 5.43% | 0.08% | -3.45% | -25.04% | 17.08% | 55.82% | -4.05% | 5.38% |
| BGR | -3.93% | 2.32% | 5.82% | -2.05% | 6.25% | 386.56% | 6.98% | -6.15% | 4.31% | -4.58% |
| BRA | 0.20% | -0.14% | -0.29% | 0.14% | -7.66% | -26.80% | -0.32% | -0.31% | 1.46% | 0.00% |
| CAN | -0.63% | 0.01% | 1.42% | -0.01% | -0.71% | -13.91% | 0.88% | -3.70% | -3.68% | -0.47% |
| CHE | -1.91% | 0.04% | 4.23% | -0.02% | -2.99% | -31.40% | 19.01% | 44.17% | -3.43% | 7.86% |
| CHN | -0.07% | 0.00% | 0.15% | 0.00% | -0.07% | -0.03% | -0.22% | 0.16% | -0.66% | 0.00% |
| CYP | -0.58% | 0.00% | 1.34% | 0.01% | 0.07% | -1.84% | -1.06% | -28.35% | -4.08% | -5.37% |
| CZE | -1.48% | 1.22% | 2.03% | -1.29% | -2.67% | 2.26% | -2.32% | -5.94% | 3.41% | 0.00% |
| DEU | -0.38% | 0.00% | 0.88% | 0.00% | -0.29% | -11.75% | 1.12% | 10.55% | -1.20% | 1.90% |
| DNK | -0.71% | -0.03% | 1.65% | 0.03% | -1.55% | -17.34% | 3.41% | 50.56% | 0.92% | 0.30% |
| ESP | -0.54% | -0.02% | 1.20% | 0.02% | -0.36% | -6.12% | 0.67% | 5.45% | -1.99% | 0.18% |
| EST | -1.10% | -0.02% | 2.54% | 0.02% | -1.54% | -14.84% | 0.75% | 39.48% | -4.84% | 0.15% |
| FIN | -0.89% | -0.02% | 2.06% | 0.01% | -1.86% | -12.98% | 2.31% | 32.48% | -1.04% | 0.09% |
| FRA | -1.16% | 0.04% | 2.53% | -0.02% | -1.80% | -19.02% | 12.71% | 23.74% | -2.30% | 4.31% |
| GBR | -0.11% | 0.12% | 0.24% | -0.09% | 0.39% | 14.80% | -6.31% | -38.58% | -2.26% | -14.53% |
| GRC | -6.08% | 4.04% | 10.10% | -3.65% | -6.33% | 463.20% | -5.56% | -32.41% | -10.05% | -31.01% |
| HRV | -4.25% | 2.39% | 6.34% | -2.09% | -3.60% | 140.14% | 7.75% | -5.84% | 2.61% | -5.38% |
| HUN | -4.27% | 2.47% | 6.42% | -2.19% | 3.80% | 271.63% | 7.67% | -5.68% | 0.95% | -4.63% |
| IDN | 2.79% | -2.17% | -4.55% | 2.06% | 6.89% | -10.38% | 10.50% | 44.55% | 13.88% | 44.85% |
| IND | 9.04% | -8.92% | -14.82% | 8.65% | 8.43% | -50.33% | 25.70% | 366.40% | 45.69% | 362.53% |
| IRL | -0.44% | 0.07% | 1.00% | -0.06% | 0.43% | 8.64% | -2.07% | -19.29% | -3.84% | -0.17% |
| ITA | -0.28% | -0.03% | 0.61% | 0.03% | -0.09% | 0.20% | -0.79% | -9.10% | -1.45% | -0.73% |
| JPN | -0.27% | 0.00% | 0.63% | 0.00% | -0.47% | -4.97% | 0.58% | 10.33% | -0.48% | 0.08% |
| KOR | -0.23% | 0.00% | 0.53% | 0.00% | -0.33% | -15.69% | 0.38% | 24.31% | -0.66% | 1.97% |
| LTU | -3.24% | 0.71% | 7.43% | -0.52% | -5.04% | -53.31% | 28.03% | -26.62% | -10.37% | 179.91% |
| LUX | 13.36% | -1.65% | -20.19% | 1.33% | 27.24% | 283.99% | -20.47% | 1.58% | 34.69% | -46.49% |
| LVA | -10.61% | 4.70% | 23.93% | -3.60% | -24.46% | -58.90% | -10.44% | -90.14% | -36.33% | -90.91% |
| MEX | -3.72% | 2.35% | 6.23% | -2.07% | 3.65% | 91.62% | -0.34% | -18.71% | -5.64% | -17.37% |
| NLD | -0.86% | -0.06% | 1.93% | 0.05% | -1.18% | -15.09% | 3.20% | 36.22% | -0.87% | 0.52% |
| NOR | -0.72% | -0.02% | 1.66% | 0.01% | -1.24% | -17.26% | 1.65% | 46.26% | -1.51% | 0.50% |
| POL | -6.87% | 3.72% | 11.13% | -3.17% | -12.63% | 92.18% | -9.07% | -37.96% | -13.45% | -36.59% |
| PRT | -1.55% | 0.22% | 3.51% | -0.15% | -2.23% | -35.74% | 25.93% | 42.70% | -3.55% | 16.11% |
| ROU | -6.78% | 3.18% | 12.52% | -2.56% | -13.78% | -27.72% | -8.77% | -50.05% | -14.60% | -49.20% |
| RUS | -6.03% | 2.84% | 12.74% | -2.20% | -13.03% | -40.58% | -13.66% | -69.10% | -27.40% | -68.46% |
| SVK | -0.57% | 0.22% | 0.81% | -0.24% | -2.38% | 0.39% | 1.25% | -0.40% | 5.24% | 0.00% |
| SVN | -1.98% | 1.68% | 2.74% | -1.79% | -4.29% | 1.93% | 0.50% | -3.81% | 3.63% | 0.00% |
| SWE | -1.25% | 0.04% | 2.79% | -0.03% | -1.29% | -11.84% | 2.95% | 23.41% | -2.13% | 0.47% |
| TUR | -0.42% | 0.01% | 0.96% | -0.01% | -0.21% | -13.10% | 0.60% | 0.65% | -1.97% | 0.77% |
| USA | 4.82% | -2.08% | -7.34% | 1.76% | 14.27% | 34.28% | 19.66% | 76.17% | 24.80% | 74.99% |

Table 2: List of countries

| ISO-3 code | Country name | ISO-3 code | Country name |
|---|---|---|---|
| AUS | Australia | IND | India |
| AUT | Austria | IRL | Ireland |
| BEL | Belgium | ITA | Italy |
| BGR | Bulgaria | JPN | Japan |
| BRA | Brazil | KOR | Republic of Korea |
| CAN | Canada | LTU | Lithuania |
| CHE | Switzerland | LUX | Luxembourg |
| CHN | China | LVA | Latvia |
| CYP | Cyprus | MEX | Mexico |
| CZE | Czech Republic | NLD | Netherlands |
| DEU | Germany | NOR | Norway |
| DNK | Denmark | POL | Poland |
| ESP | Spain | PRT | Portugal |
| EST | Estonia | ROU | Romania |
| FIN | Finland | RUS | Russian Federation |
| FRA | France | SVK | Slovakia |
| GBR | United Kingdom | SVN | Slovenia |
| GRC | Greece | SWE | Sweden |
| HRV | Croatia | TUR | Turkey |
| HUN | Hungary | USA | United States |
| IDN | Indonesia | | |

Table 3: Concordance of WIOD sectors

| WIOD description | WIOD code | Industry | WIOD description | WIOD code | Industry |
|---|---|---|---|---|---|
| Crop and animal production | A01 | Agriculture and mining | Wholesale and retail vehicles | G45 | Non-high-skilled service |
| Forestry and logging | A02 | Agriculture and mining | Wholesale trade | G46 | Non-high-skilled service |
| Fishing and aquaculture | A03 | Agriculture and mining | Retail trade | G47 | Non-high-skilled service |
| Mining and quarrying | B | Agriculture and mining | Land transport | H49 | Non-high-skilled service |
| Food products, beverages and tobacco products | C10-C12 | Food and texile | Water transport | H50 | Non-high-skilled service |
| Textiles, wearing apparel and leather products | C13-C15 | Food and texile | Air transport | H51 | Non-high-skilled service |
| Wood and cork | C16 | Resource Manufacturing | Warehousing | H52 | Non-high-skilled service |
| Paper products | C17 | Resource Manufacturing | Postal activities | H53 | Non-high-skilled service |
| Printing and reproduction of recorded media | C18 | Resource Manufacturing | Accommodation and food | I | Non-high-skilled service |
| Coke and refined petroleum products | C19 | Resource Manufacturing | Publishing | J58 | High-skilled service |
| Chemical products | C20 | Resource Manufacturing | Media | J59_J60 | High-skilled service |
| Pharmaceutical products | C21 | Resource Manufacturing | Telecommunications | J61 | High-skilled service |
| Rubber and plastic products | C22 | Resource Manufacturing | Computer and information | J62_J63 | High-skilled service |
| Other non-metallic mineral products | C23 | Resource Manufacturing | Financial services | K64 | High-skilled service |
| Basic metals | C24 | Manufacturing | Insurance | K65 | High-skilled service |
| Fabricated metal products | C25 | Manufacturing | Auxiliary to financial services | K66 | High-skilled service |
| Electronic and optical products | C26 | Manufacturing | Real estate | L68 | High-skilled service |
| Electrical equipment | C27 | Manufacturing | Legal and accounting | M69_M70 | High-skilled service |
| Machinery and equipment | C28 | Manufacturing | Architectural | M71 | High-skilled service |
| Motor vehicles | C29 | Manufacturing | Scientific research | M72 | High-skilled service |
| Other transport equipment | C30 | Manufacturing | Advertising | M73 | High-skilled service |
| Furniture | C31_C32 | Manufacturing | Other professional | M74_M75 | High-skilled service |
| Repair and installation of machinery | C33 | Non-high-skilled service | Administrative | N | High-skilled service |
| Electricity and gas | D35 | Non-high-skilled service | Public administration | O84 | High-skilled service |
| Water supply | E36 | Non-high-skilled service | Education | P85 | High-skilled service |
| Sewerage and waste | E37-E39 | Non-high-skilled service | Human health and social work | Q | High-skilled service |
| Construction | F | Non-high-skilled service | Other service | R_S | High-skilled service |